Analyst

ROYAL SOCIETY OF CHEMISTRY

PAPER

View Article Online
View Journal | View Issue

Cite this: *Analyst*, 2020, **145**, 3385

Removing interference-based effects from infrared spectra – interference fringes re-revisited†

Thomas G. Mayerhöfer, *[a,b] Susanne Pahlow,[b] Uwe Hübner[a] and Jürgen Popp[a,b]

Received 10th January 2020,
Accepted 27th March 2020

DOI: 10.1039/d0an00062k

rsc.li/analyst

Substantial refractive index mismatches between substrate and layers lead to undulating baselines, which are known as interference fringes. These fringes can be attributed to multiple reflections inside the layers. For thin and plane parallel layers, these multiple reflections result in wave interference and electric field intensities which strongly depend on the location within the layer and wavenumber. In particular, the average electric field intensity is increased in spectral regions where the reflectance is reduced. Therefore, the most important precondition for the Beer–Lambert law to hold, absorption as the single reason for electric field intensity changes, is no longer valid and, since absorption is proportional to the electric field intensity, considerable deviations from the Beer–Lambert law result. Fringe removal is consequently synonymous with correcting deviations from the Beer–Lambert law in the spectra. Within this contribution, we introduce an appropriate formalism based on wave optics, which allows a particularly fast and simple correction of any interference based effects. We applied our approach for correcting transmittance spectra of Poly(methyl methacrylate) layers on silicon substrates. The interference effects were successfully removed and correct baselines, in good agreement with the calculated spectra, were obtained. Due to its sound theoretical foundation, our formalism can be used as benchmark to test the performance of other methods for interference fringe removal.

1. Introduction

Interference is a phenomenon inherently linked to waves. If two waves have the same wavelength as well as amplitude and coincide, their superposition leads either to constructive or destructive interference. Depending on their phase relation, the resulting wave can show twice the original amplitude, be completely extinguished or anything between these two extrema. Taking light waves as an example, a typical manifestation of interference in a spectrum is the so-called interference fringes. As it was already well-known in the beginning of the twentieth century, the existence of fringes is detrimental to the evaluation of a spectrum,[1] since they can delude the spectroscopist into thinking that color is caused by absorption instead of interference (like the colors of thin oil films on water). Accordingly, Max Planck, for example, refrained from interpreting spectra of such layered materials, because he was fully aware that interference can tamper with the original color of a material and even introduce color, where there was none before.[2] Therefore, the proper removal of fringes is an important topic both in UV-Vis as well as in infrared spectroscopy.[3] In case of the latter it is even more vital, since cuvettes for liquid samples, as they are used in infrared spectroscopy, are naturally much thinner. This is because liquids are usually "colored" (meaning they are absorbing in the IR region) and require therefore much shorter path lengths compared to solutions in transparent liquids.[4] As a consequence, fringes occur in infrared spectroscopy not only in spectra of layered materials, freestanding films and those deposited on a substrate, but also in those of liquids. Over the years a number of different techniques and methods were developed to either prevent the formation of fringes or to remove them from spectra. Harrick, for instance, realized that interference is a consequence of multiple reflections inside a thin film and respectively suggested recording transmittance spectra with parallel polarized light incident under Brewster's angle.[5] Since dispersion alters the index of refraction, and thereby Brewster's angle, the results of this method are unfortunately not fully satisfying. For films on highly reflecting substrates, *i.e.* metals, the fringes are only weakly developed, since the phase shift of the light wave on the interface of metal and film is practically 180°. A closely related idea, suitable for metal substrates, is to combine light that was transmitted through and reflected from a sample, since due to energy conservation the sum of reflectance and transmittance must be unity.[6] With

[a]*Leibniz Institute of Photonic Technology (IPHT), Albert-Einstein-Str. 9, 07745 Jena, Germany. E-mail: Thomas.Mayerhoefer@leibniz-ipht.de*
[b]*Friedrich Schiller University, Institute of Physical Chemistry and Abbe Center of Photonics, Helmholtzweg 4, 07743 Jena, Germany*

†Electronic supplementary information (ESI) available. See DOI: 10.1039/d0an00062k

the advent of Fourier-Transform-IR- (FT-IR-) spectroscopy new possibilities emerged, because fringes manifest themselves ideally in a single peak in Fourier-transformed spectra. Accordingly, the pure mathematical removal of this peak appeared to be a potential solution to the fringe problem.[7] In addition, the need for computers to perform FT also allowed the direct calculation of absorbance from transmittance spectra. Since absorbances are often assumed to be additive (which, as was shown recently, is not correct[8,9]), baseline removal seemed to be possible by simple subtraction of the fringes.[10] A more advanced method based on the very same idea is the baseline/fringe removal by extended multiplicative signal correction (EMSC).[11]

A completely different way to remove fringes has been pursued in thin film optics by using wave optics theory. The rationale behind this approach is that the (Bouguer–)Beer–Lambert (BBL) law is not generally conform with wave optics. It assumes that a differential light intensity change over a differential optical path length is proportional to the intensity and that the only reason for an intensity decay is absorption. Interference, however, leads to changes of the light intensity even in the absence of absorption, since multiple reflection inside a layer lead to the existence of forward and backward traveling waves, the amplitudes of which superpose. This superposition can lead to higher intensities (constructive interference) or lower intensities (destructive interference). Depending on the ratio of wavelength and layer thickness, the average (electric field) intensity is higher at certain wavenumbers indicated by the maxima of the fringes in the transmittance spectrum, while it is lower at others. Absorption, however, is proportional to the light intensity. Given the same initial light intensity and absorption coefficient, a doubling of the path length will therefore not lead to a doubling of absorbance, in contrast to what could be expected based on the BBL law.[12,13] The principle of interference can also be exploited, among others, to enhance absorption.[14,15] The naming of the interference effect is not consistent in literature. The effect is known under various names like etaloning, cavity effect, Fabry-Pérot effect, electric field standing wave effect *etc*.

Wave optics and Maxwell's equations allow calculating the transmittance and reflectance of layer stacks, including interference effects, if the dielectric function (tensor) of substrate and film is known.[16,17] The inverse problem, *i.e.* determining the dielectric function (tensor) of the film from experimental reflectance and transmittance spectra, was also solved.[18] Correspondingly, commercial as well as free programs are available to perform the (dispersion) analysis of experimental spectra since some time.[19–21] Conveniently, this analysis encompasses the problem of fringe removal. In fact, dispersion analysis goes one important step further, as interference fringes are, from our point of view, only one manifestation of the underlying problem, the removal of which does not solve the actual problem caused by wave interference. While the removal of the interference effects by dispersion analysis or any other wave optics based approaches seems to be self-evident, this was recently verified for the correction of transflection spectra, where the impact is particularly drastic despite weakly developed interference fringes.[22] In other words, the absence of visible fringes does not mean that there are no other interference effects, that need correction.

In this contribution, we want to extend the previously described approach to remove fringes and all other interference effects from transmission spectra of layers on transparent substrates. To that end, we first examine the formation of interference effects in the layer, discuss their dependence from thickness and their influence on band positions. We then investigate how to best correct the spectra, remove the fringes and quantify the results. Since our approach is based on wave optics, it can be used in the future to benchmark other correction methods like, for example, the EMSC scheme.

2. Theoretical considerations

2.1 Calculation of the transmittance and reflectance based on the optical constants

In order to perform any wave optics conform modelling, we first have to establish an optical model, which is as close to the experiment as necessary for properly describing the experimental results (establishing the optical model is equivalent to identifying the different layers in a layer stack and determining, if the superposition of the waves is coherent or incoherent in the particular layer, so that the calculations of the electric fields can be performed[17]). Since in the infrared spectral range wavelengths are small compared to the dimensions of the sample, we assume plane waves impinging on a layer stack, which is homogeneous in the directions perpendicular to the surface normal (and within the layer) and infinite.[17,23,24] Furthermore, the light waves arrive at the layer stack from a semi-infinite incidence medium (either air or vacuum), and are partly reflected and transmitted at every interface. In addition, the part which is transmitted through the last interface enters the semi-infinite exit medium (again air or vacuum).[17,23,24] The assumption of semi-infiniteness implies for the exit medium that the waves are exclusively travelling forward and no backward travelling waves exist, which could interfere with the forward travelling wave. For the incidence medium, semi-infiniteness denotes only that the part of the wave, reflected by the layer stack and travelling in the incidence medium in reverse direction, is not again reflected. Nevertheless, in this medium, interference takes place between the incident and the reflected part of the wave. A systematic treatment, which takes into account all previous conditions, is provided by the transfer matrix method.[17,23,24]

In the following, the stack consists of a thin layer on a thick substrate. In the preceding sentence, "thin" only suggests that within the layer interference takes place, whereas the substrate is assumed to have thickness variations large enough that on average interference effects cancel. The optical model is schematically depicted in Fig. 1.

The electric field map shown in Fig. 1 was generated using the formalism provided by Centurioni[17] assuming the inci-

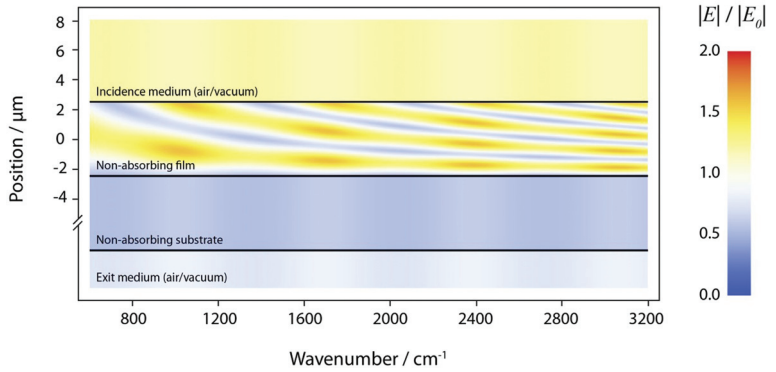

Fig. 1 Optical model of a thin layer on a substrate. Both layer as well as substrate have been assumed to be non-absorbing and to be characterized by a scalar dielectric function. For the dielectric function of the layer a wavenumber independent value of 2.1609 was assumed, whereas for the substrate we used the Sellmeier-formula with constants provided in ref. 25.

dence medium as incoherent, the coherent layer as non-absorbing with a non-dispersive dielectric constant of 2.1609 and the incoherent substrate as Si employing a Sellmeier-formula with the constants provided in ref. 25 (the assumption of the absence of interference effects in case of the substrate is justified by the fact that thickness differences on the order of the wavelength lead to the averaging out of interference effects; such an averaging out can also be caused by a decrease of the spectral resolution). While the incidence medium was considered incoherent (which has no consequence for the spectral properties of the film/substrate system), the formation of interference fringes in the 5 µm thick film is clearly visible.

From now on, we generally assume normal incidence (angle of incidence $\alpha_{\mathrm{inc}} = 0$). The transmittance T of the layer stack embedded in vacuum can then be calculated by[26]

$$\begin{aligned}
&T = \frac{T_{012}T_{20}\,\exp(-2\mathrm{Im}[\phi_2])}{1 - R_{210}R_{20}\,\exp(-4\mathrm{Im}[\phi_2])},\\
&R = R_{012} + \frac{T_{012}R_{20}T_{210}\,\exp(-4\mathrm{Im}[\phi_2])}{1 - R_{210}R_{20}\,\exp(-4\mathrm{Im}[\phi_2])},\\
&R_m = |r_m|^2, T_m = |t_m|^2,\\
&r_{210} = \frac{r_{21} + r_{10}\,\exp(2\mathrm{i}\phi_1)}{1 + r_{21}r_{10}\,\exp(2\mathrm{i}\phi_1)}, t_{012} = \frac{t_{01}t_{12}\,\exp(\mathrm{i}\phi_1)}{1 + r_{01}r_{12}\,\exp(2\mathrm{i}\phi_1)}\\
&r_{ab} = \frac{\hat{n}_a - \hat{n}_b}{\hat{n}_a + \hat{n}_b}, t_{ab} = \frac{2\hat{n}_a}{\hat{n}_a + \hat{n}_b}\\
&\phi_i(\tilde{\nu}) = 2\pi\tilde{\nu}\hat{n}_i(\tilde{\nu})d_i.
\end{aligned} \tag{1}$$

$\hat{n}_i$ is the complex index of refraction of medium i according to $\hat{n}_i(\tilde{\nu}) = n_i(\tilde{\nu}) + \mathrm{i}k_i(\tilde{\nu})$ with the real index of refraction n and the index of absorption k, all of which are usually functions of the wavenumber $\tilde{\nu}$ (eqn (1) can be derived, *e.g.*, from the transfer matrix method provided by Centurioni[17]). As already mentioned, all media are assumed to be homogeneous and characterized by a scalar dielectric function $\varepsilon(\tilde{\nu})$, for which from Maxwell's wave equation follows that $\varepsilon(\tilde{\nu}) = \hat{n}(\tilde{\nu})^2$. For the incidence and exit medium we additionally assume that $n_0 = n_3 = 1$. r_m and t_m are the reflection and transmission coefficients. In their simplest form r_{ab} and t_{ab} describe reflection from and transmission through the interface ab and are functions of the corresponding complex indices of refraction of medium a and b. ϕ_1 denote the phases of the waves within the thin film (medium 1) and the substrate (medium 2), which are functions of the wavenumber $\tilde{\nu}$, the complex indices of refraction and the thickness d of the layer. Of ϕ_2 only the imaginary part is employed, which is equivalent to neglecting interference in the substrate.[17]

2.2 Description of optical constants

For the description of the optical constants we employ the dielectric function model introduced by Kuzmenko. This model is based on a simple triangular basis function, usually at every second wavenumber point, for the imaginary part of a (principal) dielectric function.[27] For media that are characterized by scalar dielectric functions, instead of the dielectric function, also the index of absorption function can be described by the basis functions:

$$k_i(\tilde{\nu}_i) = \begin{cases} \frac{\tilde{\nu} - \tilde{\nu}_{i-1}}{\tilde{\nu}_i - \tilde{\nu}_{i-1}}, & \tilde{\nu}_{i-1} < \tilde{\nu} \le \tilde{\nu}_i \\ \frac{\tilde{\nu}_{i+1} - \tilde{\nu}}{\tilde{\nu}_{i+1} - \tilde{\nu}_i}, & \tilde{\nu}_i < \tilde{\nu} \le \tilde{\nu}_{i+1} \\ 0 & \textit{otherwise} \end{cases}. \tag{2}$$

The corresponding index of refraction function can then be obtained analytically based on one of the Kramers–Kronig relations:

$$g(x) = x\,\ln|x|. \tag{3}$$

The factor $\tilde{\nu}_i/\tilde{\nu}$ was recently introduced, because it increases the Kramers–Kronig conformity, *i.e.* the adherence to the Kramers–Kronig equations, by three orders of magnitude (in other words, the deviations between the index of refraction calculated from the right side of eqn (3) and the actual index of refraction are three orders of magnitude smaller than without the factor $\tilde{\nu}_i/\tilde{\nu}$).[28]

In contrast to Kuzmenko's suggestion, we employ the triangular basis function at every spectral point and define the values of the amplitudes A_i to be equal to the values of the

index of absorption function at the corresponding spectral points.

The complex index of refraction function is then given by:

$$\hat{n}(\tilde{\nu}_i) = n_\infty + \sum_{i=2}^{N-1} A_i(n_i(\tilde{\nu}_i) + \mathrm{i}k_i(\tilde{\nu}_i)). \quad (4)$$

N represents the number of spectral points and $n_\infty = \sqrt{\varepsilon_\infty}$, with ε_∞ being the so-called dielectric background, an offset due to the modes in the UV-Vis spectral range. Eqn (3) and (4) constitute the improved "poor man's Kramers–Kronig analysis". As has been pointed out previously,[22] the advantages over conventional Kramers–Kronig methods is the much higher flexibility in choosing the spectral points. Whereas conventional Kramers–Kronig methods usually require a constant distance between spectral points, for the poor man's Kramers–Kronig analysis the spectral points can be sparse in featureless or not interesting spectral regions.

2.3 Calculation of the corrected absorbance

The calculation of the corrected absorbance is in principle performed similarly as introduced in ref. 22. There is, however, an additional step required, which involves determining the optical constants of the substrate, since those vary depending on the doping level and the density of defects in the material.[29] This step will be described in detail at the end of this section.

In ref. 22, in a first step n_∞ and d of the thin layer were obtained in the featureless region above 3500 cm^{-1} by dispersion analysis. In the present case, we found it more convenient to preset n_∞ in order to minimize the errors of d (this is different from, *e.g.*, ref. 29 and 22, but comparable to ref. 4). In many instances n_∞ is known anyway, and if the emphasis is on removing interference effects in the optical constants for a series of spectra from layers with differing d, this strategy is preferable (whenever the determination of optical constants has priority, we would recommend classical dispersion analysis). Correspondingly, we fit the transmittance in the spectral region above 3500 cm^{-1} assuming a constant index of refraction equal to n_∞ and vary only d iteratively to minimize the deviations between experimental and simulated values.

After d has been determined, a first estimation of the absorption index is calculated. To that goal, we use n_∞ and d to calculate a transmittance spectrum $T_{\mathrm{calc}}(\tilde{\nu}, d, n_\infty)$ assuming that the layer is non-absorbing. From the experimental transmittance spectrum, we then obtain this first estimation for k by:

$$k_{\mathrm{app}}(\tilde{\nu}) = -\frac{\ln 10}{4\pi \mathrm{d}\tilde{\nu}} \log_{10}\left(\frac{T_{\mathrm{meas}}(\tilde{\nu})}{T_{\mathrm{calc}}(\tilde{\nu}, d, n_\infty)}\right). \quad (5)$$

This somewhat naïve way of fringe removal is similar to that suggested by Clark and Moffatt.[10] The difference to their approach is that we use the baseline correction at this stage only to achieve better initial estimates for the absorption index function like in ref. 22. As already stated, just removing fringes cannot correct effects like dispersion distortion, band shifts or intensity changes based on the interference effects.[22]

After having obtained the first estimate for the index of absorption function $k_{app}(\tilde{\nu})$, eqn (2)–(4) are employed to generate first values for $\hat{n}(\tilde{\nu})$ and, by applying eqn (1), for $A_{\mathrm{calc}} = -\log_{10} T_{\mathrm{calc}}$.

Afterwards, $k(\tilde{\nu})$ is iteratively improved. The first couple of iterations use the correction suggested by Tonoue *et al.*:[30]

$$k_{i+1}(\tilde{\nu}) = k_i(\tilde{\nu}) \frac{A_{\mathrm{meas}}(\tilde{\nu})}{A_{\mathrm{calc},i}(\tilde{\nu})}. \quad (6)$$

In the beginning, this correction leads to the strongest improvements. However, it can cause spikes and usually converges too fast. Therefore, after convergence has reached, the correction suggested by Hawranek *et al.* is employed:[4]

$$k_{i+1}(\tilde{\nu}) = k_i(\tilde{\nu}) + \frac{\ln 10}{4\pi \mathrm{d}\tilde{\nu}} (A_{\mathrm{calc},i}(\tilde{\nu}) - A_{\mathrm{meas}}(\tilde{\nu})). \quad (7)$$

In contrast to the scheme for transflection spectra, eqn (7) will mostly be sufficient to arrive at satisfactorily corrected absorbance values. Therefore, no further correction procedures are necessary.

Coming back to the determination of the optical constants of the Si waver, it is performed analogously to those of the films. However, the initial steps are different. First of all, we use the literature values for the index of refraction function[25] to calculate a reflectance spectrum from eqn (1) (setting the layer thickness $d = 0$). From the sum of calculated reflectance and experimental transmittance we calculate a first estimation of the index of absorption function by:

$$k_{\mathrm{app,Si}}(\tilde{\nu}) = -\frac{\ln 10}{4\pi d_{\mathrm{Si}} \tilde{\nu}} \log_{10}\left[T_{\mathrm{meas,Si}}(\tilde{\nu}) + R_{\mathrm{calc,Si}}(\tilde{\nu})\right]. \quad (8)$$

From this point on, the determination of the optical constants follows exactly the same path as for the PMMA layers. The corresponding results are illustrated in ESI Fig. 1.†

Fig. 2 displays the complete algorithm in a flow chart.

This algorithm was translated into a program using Mathematica 10.2 and its compiled functions to speed up the numerical evaluation of the equations (no further optimizations were employed). The calculations were carried out on a typical office PC (i5-6500 CPU@3.2 GHz) and usually took about a minute.

3. Experimental details

3.1 Preparation of the samples

A double-side polished Si wafer (orientation ⟨100⟩, thickness 525 μm, resistivity > 10.000 Ohm cm) was spin coated with a photoresist to protect the surface during the subsequent cutting process. Finally, the wafer was sliced in squares with a size of 12.7 × 12.7 mm^2.

Afterwards, the chips were cleaned by removing the photoresist with organic solvents (acetone bath and rinse in isopropanol) followed by a bath in Caro's acid (peroxymonosulfuric acid) to remove all organic residuals. After the cleaning procedure, a poly(methyl methacrylate) (PMMA) resist was spin-

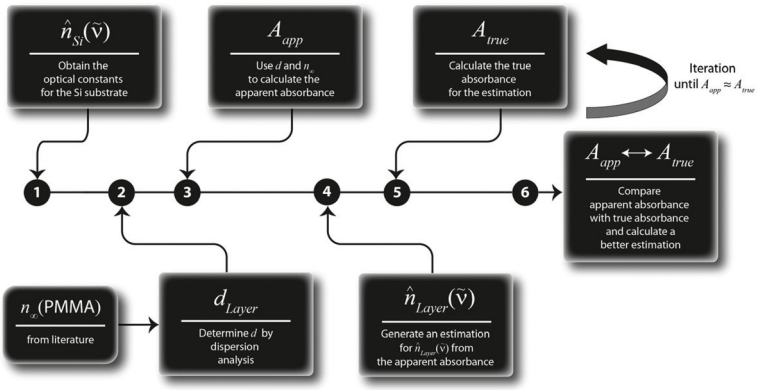

Fig. 2 Flow chart illustrating the algorithm used to determine the corrected index of absorption function/the corrected absorbance.

coated on the individual chips with film thicknesses between 1000 and 2000 nm and dried for 10 min at 180 °C on a hotplate. The PMMA electron beam resist "ARP 672.11" was purchased from the Allresist GmbH Berlin.

3.2 Infrared measurements

The infrared measurements were carried out on a Bruker Vertex 80v FT-spectrometer with a spectral resolution of 4 cm^{-1} (interpolated 1 cm^{-1}). For the first series of measurements a conventional transmittance accessory and the corresponding deuterated L-α-Alanine-Doped Triglycine Sulfate (DLaTGS) detector was employed. As can be seen in ESI Fig. 2,† the spectrum of the pure Si substrate shows a surprising behavior on the first view with regard to the baseline for the spectral range above about 3500 cm^{-1}. The expectation would be a nearly constant transmittance in this range. (A corresponding curve, based on literature values,[25] of the index of refraction function can also be found in ESI Fig. 2.†) The reason for these deviations above 3500 cm^{-1} is the beam, which is usually focused in the sample. If a substrate is used, the focal point is changed and, as a result, parts of the beam will not hit the detector. According to Bruker, a solution is the use of a parallel beam unit combined with a proper detector element. Therefore, we also conducted measurements with Bruker's A 480/8 unit with the corresponding DLaTGS detector with a larger detector element. Unfortunately, even then spectra with a correct baseline were not obtained (*cf.* ESI Fig. 2†) and adjusting the accessory also did not improve the result. We therefore decided to combine our spectra from both measurement series. For the range from 500–3450 cm^{-1} we used the spectra recorded with the conventional transmittance accessory without any corrections. For the range from 3450–7500 cm^{-1}, we employed the spectra recorded with the A 480/8 unit. To compensate for the too strong slope with increasing wavenumber, we calculated a slope correction for the uncoated Si substrate, so that the slope of its spectrum and the absolute values were adapted to the transmittance calculated by eqn (1) from the literature values[25] (*cf.* ESI Fig. 3†).

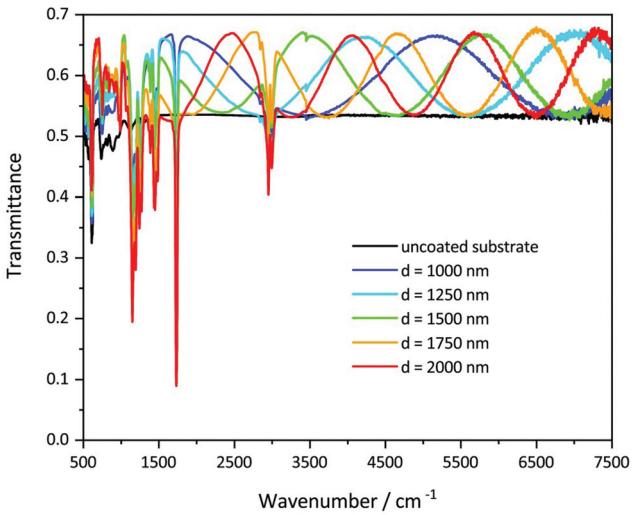

Fig. 3 Corrected experimental transmittance spectra. In the range from 500–3450 cm^{-1} the spectra (recorded with conventional transmittance accessory) remained uncorrected, while in the region between 3450–7500 cm^{-1} (acquired with A 480/8 unit) their baseline was adapted according to eqn (9).

Accordingly, all spectra of the coated substrates were corrected in the range 3450–7500 cm^{-1} with the same formula:

$$T_{corr}(\tilde{\nu}) = T_{meas}(\tilde{\nu}) + 9.095\times10^{-6}\times\tilde{\nu} - 0.0721. \quad (9)$$

The resulting spectra are depicted in Fig. 3. Note that, one criterion for the quality of the correction is that in non-absorbing regions and for substrates with a larger ε_∞ than the coatings, the minima of the fringes should touch the transmittance of the bare substrate. This condition is obviously fulfilled after applying our correction scheme.

4. Results and discussion

4.1 General preliminary remarks

We have emphasized several times that the sole removal of fringes does not solve the underlying problem caused by inter-

ference, which consists in the varying electric field intensity and, since absorption is proportional to this intensity, the corresponding variation of absorption.[12,13,31] As was already illustrated in Fig. 1, the electric field is strongly changing in the layer on top of a Si substrate as a function of the z-coordinate (the film depth) and the wavenumber. However, the film displayed in Fig. 1 is non-absorbing and absorption certainly also influences the electric field strength. We have therefore recalculated the electric field map shown in Fig. 1, assuming a medium with the same dielectric background ε_∞, but with comparably weak absorption bands every 200 cm^{-1}, which is displayed in Fig. 4. (All oscillators have the same oscillator strength. The corresponding index of refraction and absorption functions can be found in ESI Fig. 4.†) If we calculate the corresponding transmittance spectrum, divide it by the transmittance of a blank, take the negative decadic logarithm and divide by the thickness of the layer, an apparent decadic absorption coefficient a_{app} (often called "absorptivity", but we will comply with the IUPAC recommendations) results,

$$a_{app}(\tilde{\nu}) = \frac{-\log_{10}\left(\frac{T_{meas}(\tilde{\nu})}{T_{calc}(\tilde{\nu}, d, n_\infty)}\right)}{d}, \quad (10)$$

which varies by ±80 cm^{-1}. Note that the blank consists of a non-absorbing layer, having the same n_∞ as the absorbing layer, placed on the same substrate. Therefore, the variations of $a_{app}(\tilde{\nu})$ are caused only by the electric field variations and are not due to the fringes. In this context, we want to point out, that it is not absorbance that is proportional to the electric field strength, but absorptance (= $1 - R - T$).[18,19] In the following, we would like to briefly explain the problems associated with the most commonly used definition of the quantity absorbance. According to its common definition, absorbance should not be a function of the electric field strength, since all changes of the electric field strength should be due to absorption. Accordingly, the electric field intensity E^2 is replaced by intensity I,

$$\begin{aligned} &dI = -\alpha(\tilde{\nu})E(\tilde{\nu}, x, y, z)^2 dl \rightarrow \\ &dI = -\alpha(\tilde{\nu})dl \rightarrow\rightarrow \\ &A = -\log_{10}\left(\frac{I}{I_0}\right) = a(\tilde{\nu})d \quad a(\tilde{\nu}) = \alpha(\tilde{\nu}) \cdot \log_{10} e, \end{aligned} \quad (11)$$

and the decadic absorption coefficient spectrum $a(\tilde{\nu})$ is supposed to be a specific quantity. By means of an example we will show that the definition of absorbance according to eqn

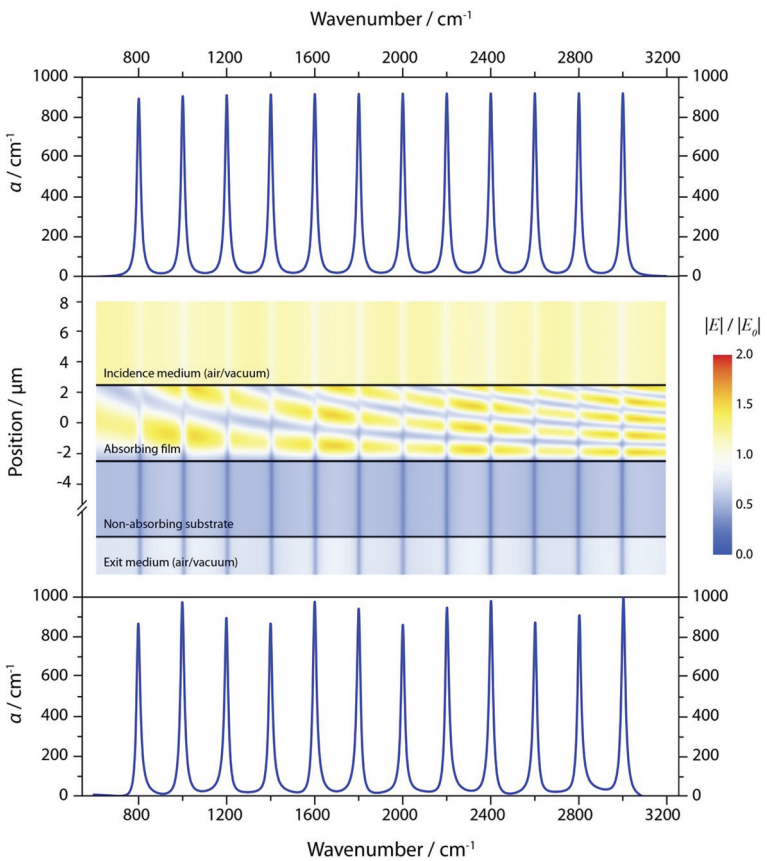

Fig. 4 Top section: Decadic absorption coefficient spectra of the artificial medium used for the layer. Medium section: Electric field map of the layer on top of the Si-substrate. The layer consisting of the artificial medium is located between 2.5 and –2.5 μm. Lower part: Apparent decadic absorption coefficient that results after a baseline correction by which the transmittance of the sample was divided by the transmittance of a non-absorbing layer having the same n_∞ and thickness d placed on the same substrate.

(11) is unfortunately fundamentally flawed in practice and not compatible with Maxwell's equations, except under very restricting circumstances.[32]

Fig. 4 illustrates the effects of interference on the apparent absorption coefficient. In particular, the regions between the peaks of the apparent absorption coefficient spectrum show that the peaks themselves are no longer symmetric. This is due to the fact that the change in intensity is governed by both, the absorption coefficient (in this case the specific version calculated from the material property, *i.e.* the dielectric function) and the electric field intensity. Therefore, if the electric field intensity maximum is close to the peak value of the absorption coefficient, it is also possible that the absorbance peak value is not located at the maximum of the absorption coefficient. Note that the absorption index maximum and, with it, the absorption coefficient maximum, is anyway generally not located at the oscillator position. This is a consequence of the relation $k = \varepsilon''/2n$. Accordingly, for the index of absorption function, the symmetric bands of the imaginary part of the dielectric function become modulated by dispersion around the bands yielding shifts of the band maxima to higher wavenumbers, away from the oscillator position.[8,9]

To estimate the band shifts and the peak intensity changes in dependence of the PMMA thickness, we used the literature values for the Sellmeier parameters of the Si substrate[25] and the oscillator parameters for PMMA provided in ESI Table 1.† The results are shown in Fig. 5 and compared to those of the same calculations under negligence of interference (but multiple reflections within the layer are still taken into consideration). First of all, we note deviations of the apparent absorption coefficient of up to ±20%. Furthermore, the changes have a periodic character with an underlying exponential decay due to absorption. The periodicity remains the same as the electric field intensity changes and is out of phase for different peaks. Because instead of the absolute peak intensities often relative peak intensities are employed, due to the different periodicity of the peaks, the relative peak ratio changes can amount up to ±40%. The peak shifts have the same periodicity as the intensity changes and can be as high as 4 cm^{-1}. On average the peak shifts have the same value as in the incoherent case. Overall, they are much weaker than their counterparts in transflectance spectra,[13,22] but they are still strong enough to be realized in experimental spectra and a proper correction scheme should not only take care of the intensity changes, but should also be capable of removing the peak shifts. In this respect, please note, that to remove the fundamental shift as well, it would be necessary to calculate the imaginary part of the dielectric function from the corrected absorption and refractive index functions and to determine the peak positions. Alternatively, dispersion analysis can be applied as a correction scheme, which is able to determine the correct oscillator positions directly.[33]

4.2 Evaluation of the experimental transmission spectra of PMMA layers on Si

As detailed in section 2.3, the first step of the correction scheme is to fit the non-absorbing region from 3500–7500 cm^{-1} assuming a fixed $n_\infty = 1.47$. Accordingly, the only variable parameter is the thickness d. The fits took on average about 3 seconds and the deviations between nominal and modelled layer thickness are between 1 and 5% (*cf.* Fig. 6 and Table 1).

In the next step, eqn (10) is applied and an apparent absorption coefficient spectrum is calculated for each sample. The result is displayed in Fig. 7 (the ratio of the spectra $T_{meas}(\tilde{\nu})/T_{calc}(\tilde{\nu}, d, n_\infty)$ can be found in ESI Fig. 5†). If the spectra followed the Beer–Lambert law strictly, the expectation would be that the thickness dependence was removed and the absorption coefficient was the same for all five spectra. In contrast, if the wave optics based calculation, according to Fig. 5,

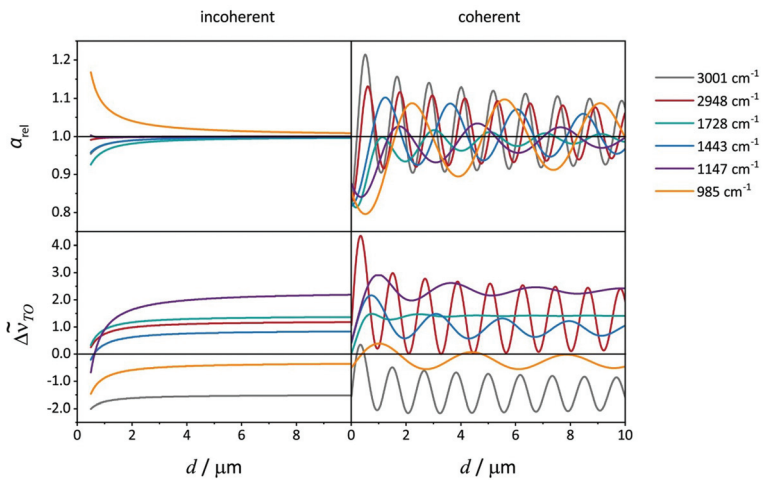

Fig. 5 Upper part: Dependence of the relative apparent absorption coefficient peak values on the PMMA layer thickness (unity value would indicate agreement between apparent and true value). Lower part: Dependence of the relative peak position changes on the PMMA layer thickness (zero would indicate agreement between peak and oscillator position). Left side: Thickness dependence if interference effects would be neglected. Right side: Fully coherent calculation.

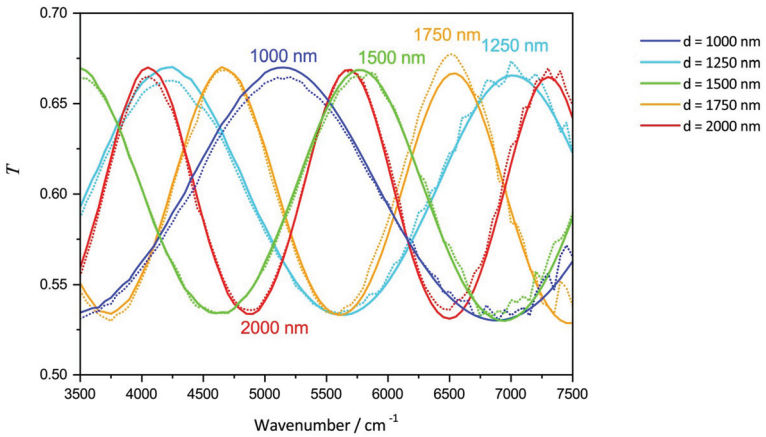

Fig. 6 Fit of the experimental transmission spectra of PMMA layers on Si assuming a fixed constant and real refractive index (dashed line) and comparison with the modelled transmission spectra (solid line).

Table 1 Values of d_{calc} as obtained by the fitting procedure of the experimental spectra as well as the time necessary for the evaluation

d/nm	n_∞	d_{calc}/nm	t/s
1000	1.47	990	2.8
1250	1.47	1221	2.6
1500	1.47	1472	2.8
1750	1.47	1819	3.0
2000	1.47	2094	3.6

upper right part, is applied, deviations of about ±10% should occur in the thickness range 1 μm ≤ d ≤ 2 μm. The experimental results indeed show variations of this order, as can be seen in Fig. 7, which is already strong evidence that the wave optics based calculation is correct. Apart from these deviations, these calculations also predict noticeable changes of the band positions.

For the band at about 2950 cm^{-1}, the wave optics based approach predicts that its peak should be nearly at the oscillator position for d ≈ 1 μm and 2 μm, while the maximum deviation is expected at d ≈ 1.5 μm, which agrees with what can be found in Fig. 8, lower part. The absolute deviation is, however, somewhat less than the predicted 3 cm^{-1}, which is related to the fact that this spectral region could not be fitted satisfactorily assuming one oscillator. Further, the prediction certainly is also influenced by the error of the optical constants. The oscillator at about 2995 cm^{-1} is also expected to show the strongest blue shift for d ≈ 1.5 μm, which can also be seen in the experimental data. For this oscillator, the maximum shift is expected to be about 1 cm^{-1}, which is confirmed by the experimental data.

From a suitable correction scheme, we would demand to remove both, the deviations concerning the absorption coefficient as well as the spectral shifts. In fact, after application of

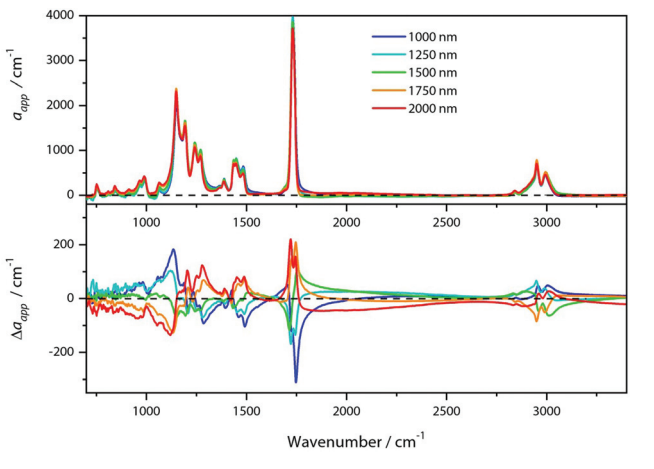

Fig. 7 Upper part: Absorption coefficient spectra of the PMMA layers on Si after simple baseline correction. Lower part: Variation of the absorption coefficient relative to the average value of all five samples.

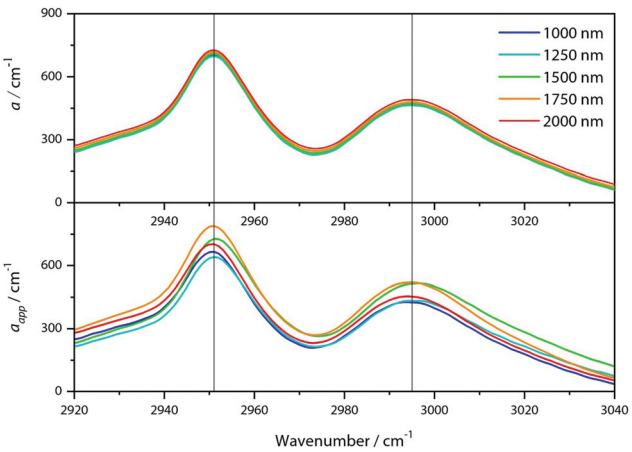

Fig. 8 Lower part: Apparent absorption coefficient spectra of the PMMA layers on Si after simple baseline correction in the range between 2920 and 3040 cm^{-1}. Upper part: Same as lower part but after the wave optics-based correction scheme.

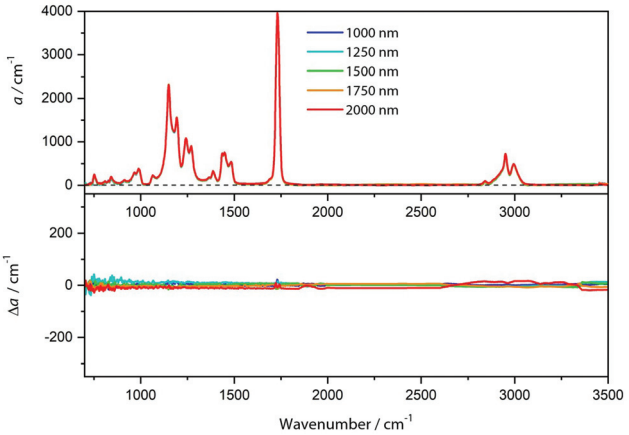

Fig. 9 Absorption coefficient spectra of the PMMA layers on Si after application of the wave optics based correction scheme. Lower part: Variation of the absorption coefficient relative to the average value of all 5 layers.

the wave optics based correction scheme, which took about a minute for one spectrum, all absorption coefficient spectra agree within linewidth as can be seen in Fig. 9. The remaining deviations are about an order of magnitude smaller and consist mainly of errors due to the baseline correction. Nevertheless, even these errors have been clearly reduced when we compare Fig. 7 with Fig. 9. In addition, the baseline is after proper correction nowhere negative, in contrast to the baselines after the simple correction scheme. Furthermore, the band shifts and the band shape changes have been corrected, which is in particular obvious from the comparison provided in Fig. 8. In addition, dispersion effects, eminently visible at the high wavenumber side of the bands in Fig. 7, have also been removed.

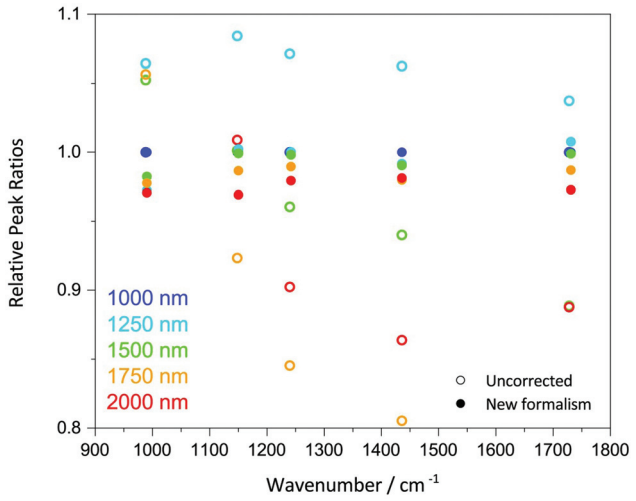

Fig. 10 Band ratios relative to the band at about 2950 cm^{-1} for the uncorrected experimental absorption coefficient spectra in comparison with those obtained by the wave optics-based formalism.

A last step for assessing the value of the wave optics based correction scheme is the comparison of the relative band ratios. As already discussed, since usually the interference effects are out of phase for two bands, the errors can add up if one band is at the maximum decrease and the other at the maximum increase of absorption.

In particular the relative band ratio α (1440 cm^{-1})/α (2952 cm^{-1}) shows enormous variations between 0.81 and 1.06 before the correction, while the variations are reduced to 0.98–1.0 afterwards. In general, the band ratio changes are not larger than ±2% after the correction (Fig. 10).

5. Summary and conclusions

We showed that the correction of interference effects in layers on transparent substrates requires more than just the removal of the interference fringes. We demonstrated that interference causes reduced or enhanced absorption and is responsible for errors of the absorption coefficients, which need to be addressed. In particular, this is necessary for spectral ranges with absorption bands since shifts of the maxima and dispersion related band shape changes will occur due to interference as well. Our correction scheme comprises all interference based effects and therefore can be considered as benchmark system. We consider the successful execution of these corrections as benchmarks. We would encourage that other procedures used to remove fringes should undergo tests to assess to what extent they are able to remove or correct all of the interference-related effects. Certainly, in special cases, when, for instance, only approximate band positions are of interest, the application of less elaborate procedures might be fully sufficient. On the other hand, it can be only of advantage to precisely know under which conditions what method can be applied. Since all of the effects lead to deviations from the Beer–Lambert law, benchmarking would not only be of practical interest, but also help to better narrow down its limits and evaluate, if or when its approximations are still valid or a changeover to wave optics is necessary.

Conflicts of interest

There are no conflicts of interest to declare.

Acknowledgements

Financial support of the EU, the "Thüringer Ministerium für Wirtschaft, Wissenschaft und Digitale Gesellschaft", the "Thüringer Aufbaubank", the Federal Ministry of Education and Research, Germany (BMBF) for the research projects "Intersept" (13N13852), "EXASENS" (13N13856) and "InfectoGnostics" (13GW0096F), the German Science Foundation, the "Fonds der Chemischen Industrie" and the Carl-Zeiss Foundation is gratefully acknowledged.

References

1 C. Lutinski, *Anal. Chem.*, 1958, **30**, 2071–2072.
2 M. Planck, *Sitzungsberichte der Königlich Preussischen Akademie der Wissenschaften*, 1903, vol. I, pp. 480–498.
3 R. W. Burnett, *Anal. Chem.*, 1973, **45**, 383–385.
4 J. P. Hawranek, P. Neelakantan, R. P. Young and R. N. Jones, *Spectrochim. Acta, Part A*, 1976, **32**, 85–98.
5 N. J. Harrick, *Appl. Spectrosc.*, 1977, **31**, 548–549.
6 P. J. Farrington, D. J. T. Hill, J. H. O'Donnell and P. J. Pomery, *Appl. Spectrosc.*, 1990, **44**, 901–903.
7 T. Hirschfeld and A. W. Mantz, *Appl. Spectrosc.*, 1976, **30**, 552–553.
8 T. G. Mayerhöfer and J. Popp, *ChemPhysChem*, 2019, **20**, 511–515.
9 T. G. Mayerhöfer and J. Popp, *Spectrochim. Acta, Part A*, 2019, **215**, 345–347.
10 F. R. S. Clark and D. J. Moffatt, *Appl. Spectrosc.*, 1978, **32**, 547–549.
11 T. Konevskikh, A. Ponossov, R. Blumel, R. Lukacs and A. Kohler, *Analyst*, 2015, **140**, 3969–3980.
12 T. G. Mayerhöfer, H. Mutschke and J. Popp, *ChemPhysChem*, 2017, **18**, 2916–2923.
13 T. G. Mayerhöfer and J. Popp, *Spectrochim. Acta, Part A*, 2018, **191**, 283–289.
14 T. G. Mayerhöfer and J. Popp, *Spectrochim. Acta, Part A*, 2018, **191**, 165–171.
15 S. Pahlow, T. Mayerhöfer, M. van der Loh, U. Hubner, J. Dellith, K. Weber and J. Popp, *Anal. Chem.*, 2018, **90**, 9025–9032.
16 F. Abelès, *Ann. Phys.*, 1950, **12**, 596–640.
17 E. Centurioni, *Appl. Opt.*, 2005, **44**, 7532–7539.
18 O. Stenzel, *The Physics of Thin Film Optical Spectra: An Introduction*, Springer International Publishing, 2015.
19 https://wtheiss.com/.
20 https://sites.google.com/site/reffitprogram/home.
21 http://www.shportko.com/products.html.
22 T. G. Mayerhöfer, S. Pahlow, U. Hübner and J. Popp, *Analyst*, 2018, **143**, 3164–3175.
23 P. Yeh, *Optical Waves in Layered Media*, Wiley, 2005.
24 M. Born, E. Wolf and A. B. Bhatia, *Principles of Optics: Electromagnetic Theory of Propagation, Interference and Diffraction of Light*, Cambridge University Press, 1999.
25 D. Chandler-Horowitz and P. M. Amirtharaj, *J. Appl. Phys.*, 2005, **97**, 123526.
26 O. Stenzel, V. Hopfe and P. Klobes, *J. Phys. D: Appl. Phys.*, 1991, **24**, 2088.
27 A. B. Kuzmenko, *Rev. Sci. Instrum.*, 2005, **76**, 083108.
28 T. G. Mayerhöfer and J. Popp, *Spectrochim. Acta, Part A*, 2019, **213**, 391–396.
29 S. W. King and M. Milosevic, *J. Appl. Phys.*, 2012, **111**, 073109.
30 R. Tonoue, M. Katsura, M. Hamamoto, H. Bessho and S. Nakashima, *Appl. Spectrosc.*, 2014, **68**, 733–739.
31 M. Milosevic and S. W. King, *ECS J. Solid State Sci. Technol.*, 2015, **4**, N3146–N3152.
32 T. G. Mayerhöfer, H. Mutschke and J. Popp, *ChemPhysChem*, 2016, **17**, 1948–1955.
33 T. G. Mayerhöfer and J. Popp, *ChemPhysChem*, 2019, **20**, 31–36.